

Supporting Information

All-Solid-State Supercapacitors Using A Highly-Conductive Neutral Gum Electrolyte

Nengsheng Yu,^{a,b,c} Xiaona Wang^a, Silan Zhang^a, Sha Zeng,^a Yongyi Zhang,^{a,c} Jiangtao Di,^{a,c*}
Qingwen Li^{a,c}

a Suzhou Institute of Nano-Tech and Nano-Bionics, Chinese Academy of Sciences, Suzhou 215123, People's Republic of China. E-mail: jtdi2009@sinano.ac.cn;

b Nano Science and Technology Institute University of Science and Technology of China, Suzhou 215123, China.

c Division of Nanomaterials, Suzhou Institute of Nano-Tech and Nano-Bionics, Nanchang, Chinese Academy of Sciences, Nanchang 330200, China

Deposition potential	0-0.6V	0-0.8V	0.3-0.6V	0.3-0.8V	0.3-1V
Mass density(mg/cm^2)	0.53	0.51	0.52	0.75	0.71

Tab. S1 Mass density of MnO_2/CNT films at different deposition potential.

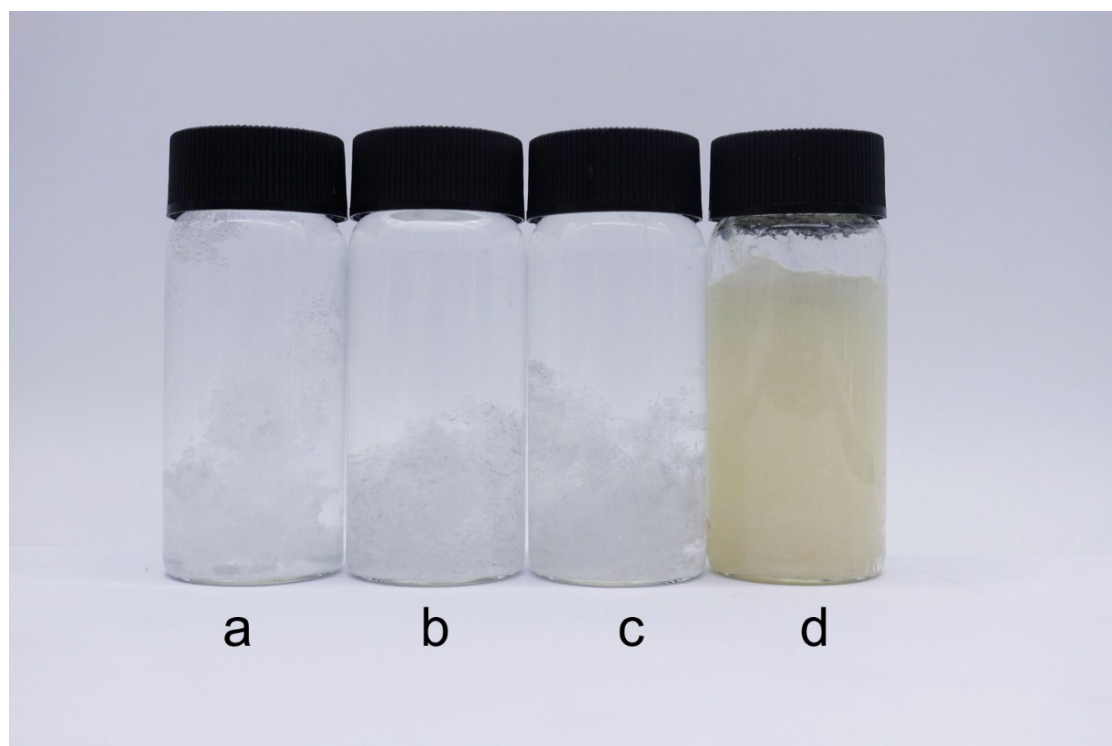


Fig. S1 Optical images of 20 wt% of PVA with (a) 0.1 M, (b) 0.5 M, (c) 3 M of Na_2SO_4 ; (d) Optical image of 20 wt% xanthan gum with 3 M of Na_2SO_4 .

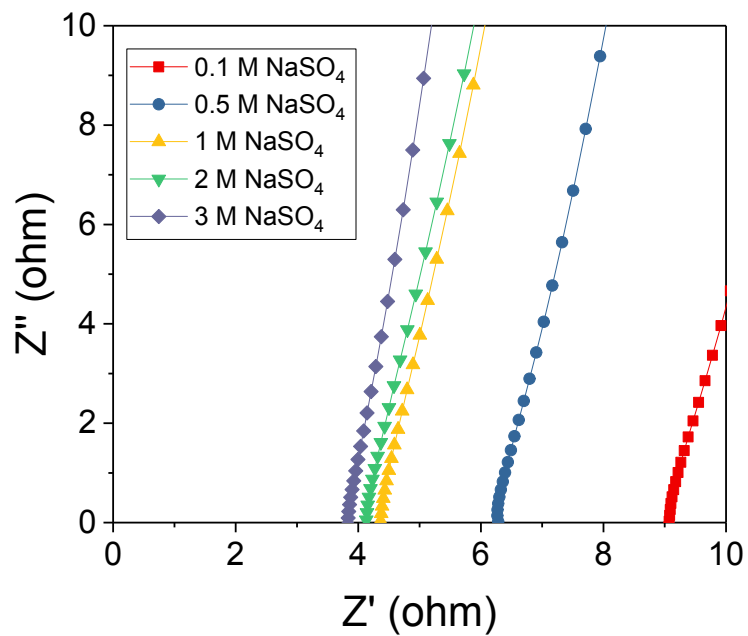


Fig. S2 AC impedance spectra of the xanthan gum electrolytes containing 20 wt% xanthan gum with different concentrations of sodium sulfate.

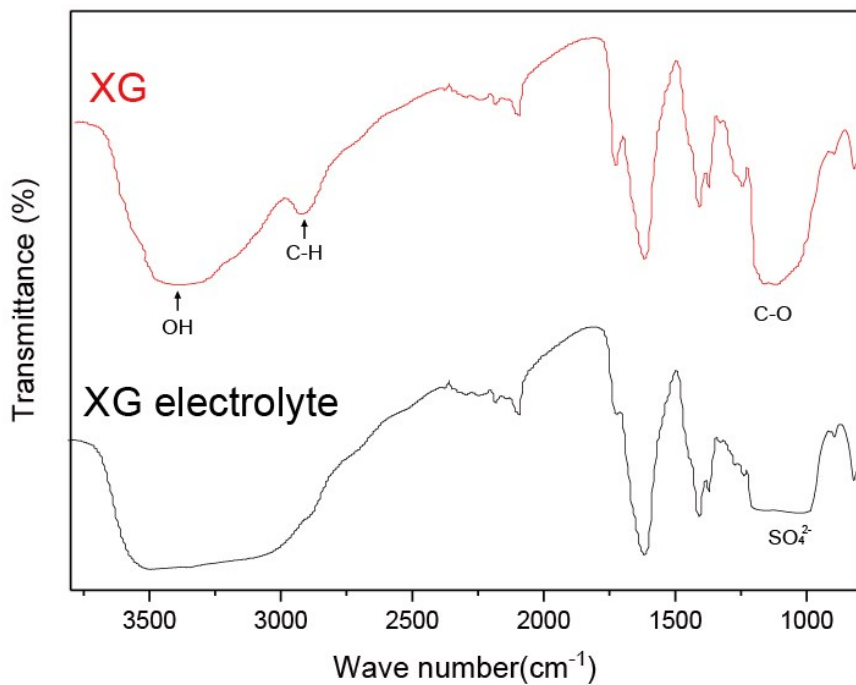


Fig. S3 IR spectra of xanthan gum and the Na_2SO_4 /xanthan gum electrolyte.

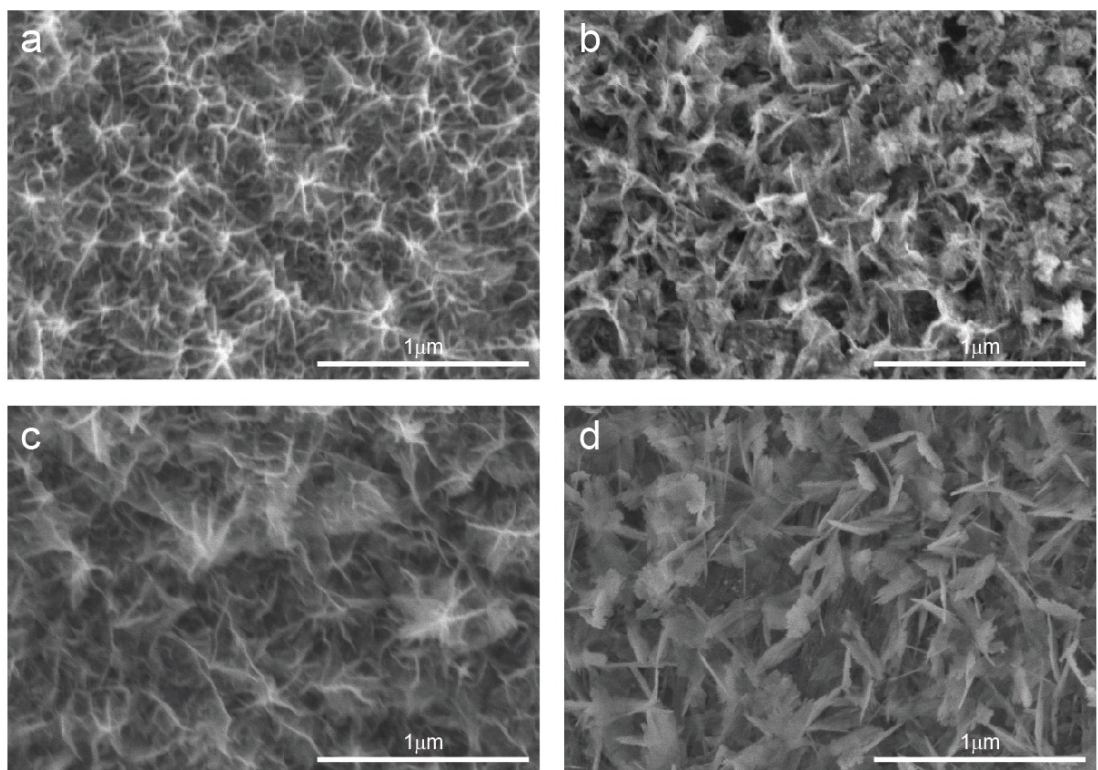


Fig. S4 SEM image of MnO_2 at different deposition potential. a) $\text{MnO}_2\text{-1}$; b) $\text{MnO}_2\text{-2}$; c) $\text{MnO}_2\text{-4}$; d) $\text{MnO}_2\text{-5}$.

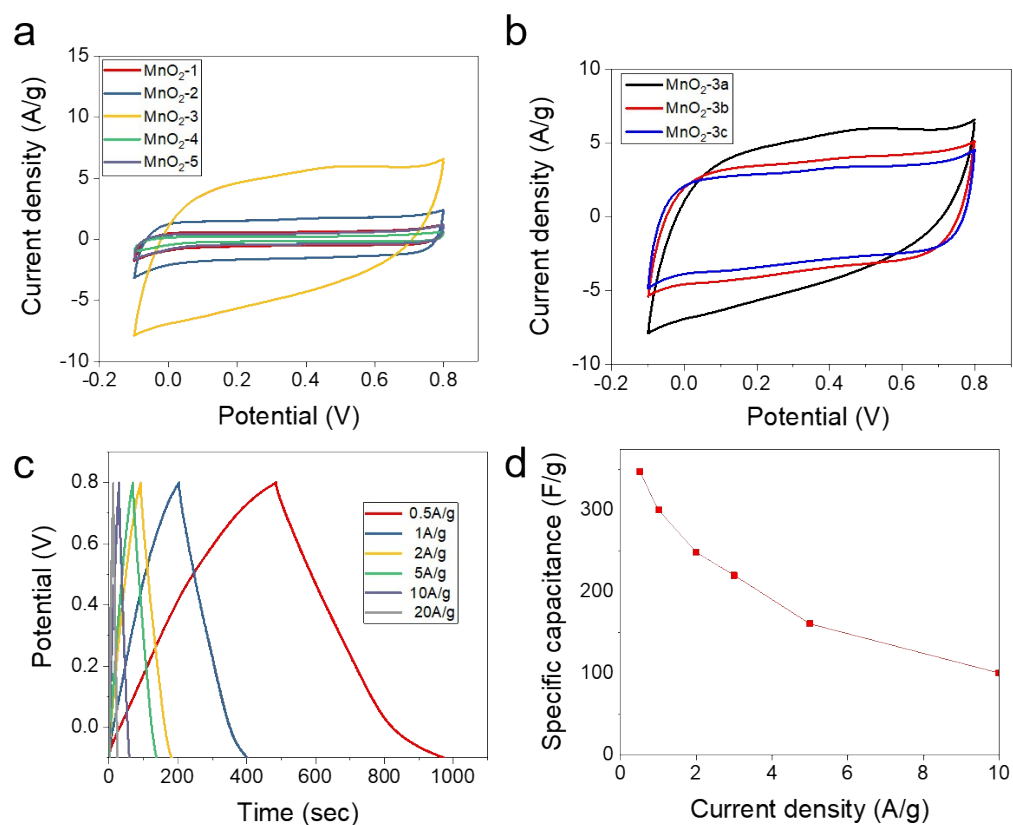


Fig. S5 Electrochemical measurement of MnO_2/CNT films with 1 M Na_2SO_4 aqueous solution as the electrolyte. a) CV curves of obtained at 5mV/s at different deposition scan

rates ($\text{MnO}_2\text{-1}$: +0.3 V and +0.6 V; $\text{MnO}_2\text{-2}$: +0.3 V and +0.8 V; $\text{MnO}_2\text{-3}$: +0.3V and +1.0 V; $\text{MnO}_2\text{-4}$: 0 V and +0.8 V; $\text{MnO}_2\text{-5}$: 0 V and +0.6 V) ; b) CV curves obtained at 5mV/s at different deposition potential ($\text{MnO}_2\text{-3a}$:250 mV/s, $\text{MnO}_2\text{-3b}$: 50 mV/s, $\text{MnO}_2\text{-3c}$:100 mV/s.); c) GCD curves of $\text{MnO}_2\text{-3a}$ /CNT films at different current density; d) Rate performance of $\text{MnO}_2\text{-3a}$ /CNT.

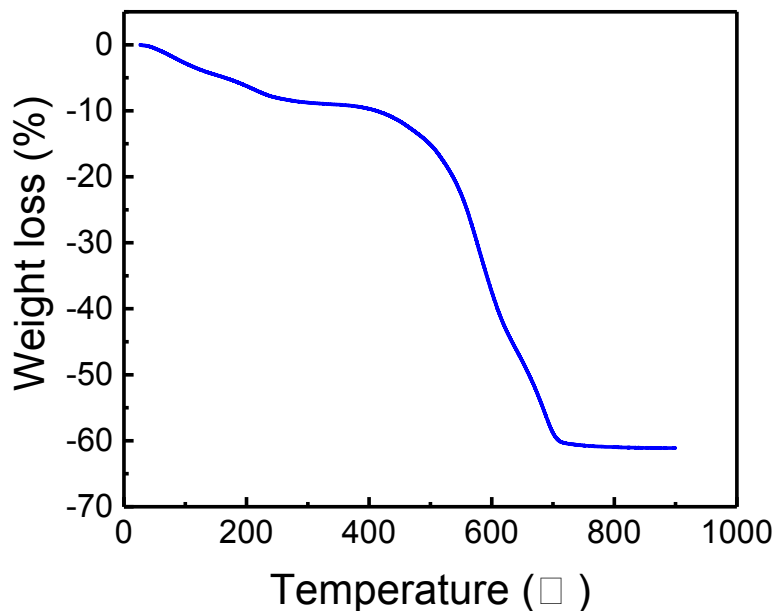


Fig. S6 TGA of MnO_2 /CNT films

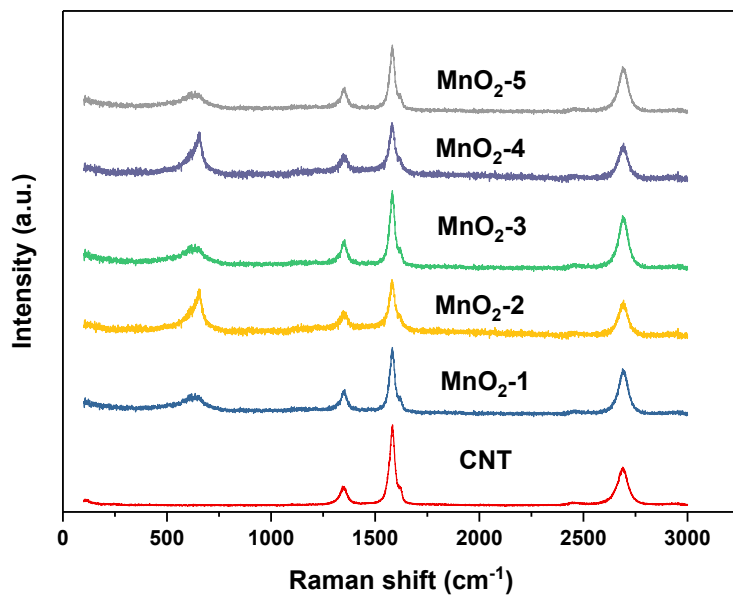


Fig. S7 Raman spectra of MnO_2 /CNT films at different deposition potential.

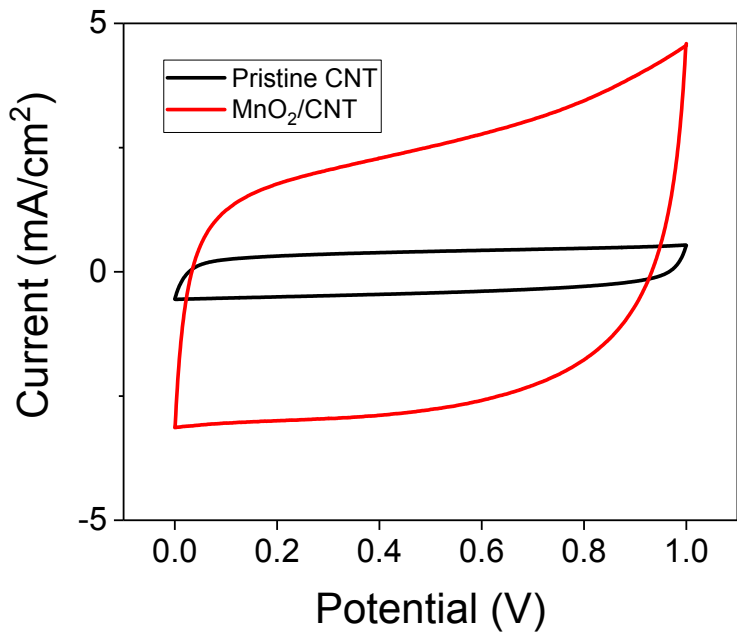


Fig. S8 CV curves (scan rate: 2 mV/s) of the flexible supercapacitors based on pristine CNT and MnO₂/CNT electrodes.

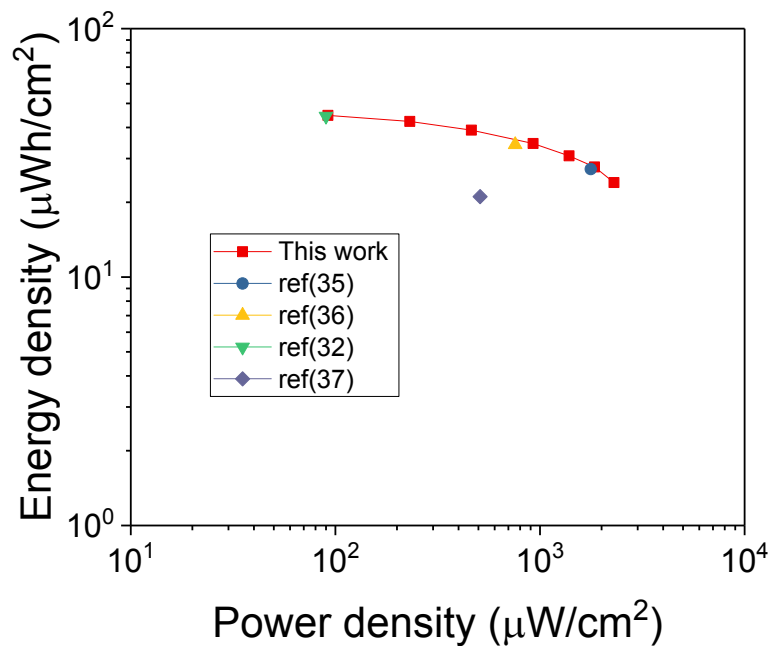


Fig. S9 Ragone plots of all-solid-state supercapacitor based on MnO₂/CNT electrodes.

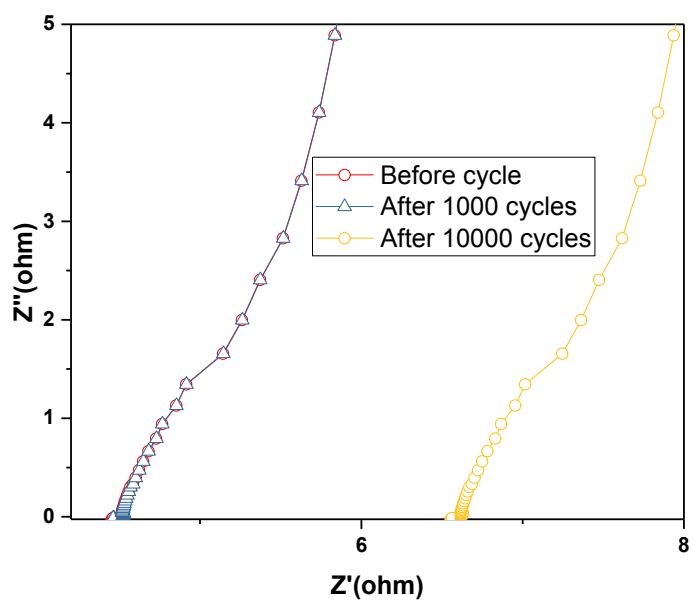


Fig. S10 Nyquist plot of all-solid-state supercapacitors at different cycle number.